UV-Induced Gelation on Nanometer Scale Using Liposome Reactor

Sergey Kazakov, Marian Kaholek, Iwao Teraoka, and Kalle Levon*

Department of Chemistry, Chemical Engineering, and Materials Science, Polytechnic University, Six MetroTech Center, Brooklyn, New York 11201

Received September 21, 2001; Revised Manuscript Received December 5, 2001

ABSTRACT: A protocol for preparation of polymer hydrogel spherical particles on a nanometer scale (nanogels) was developed. The protocol includes encapsulation of hydrogel-forming components into liposomes, UV-induced polymerization within the liposomes, solubilization of the lipid bilayer by detergent, removal of the phospholipid, detergent molecules, and their micelles by dialysis, and drying nanogels by evaporation in a temperature gradient. Dynamic light scattering technique was employed to characterize the size distribution of poly(acrylamide), poly(*N*-isopropylacrylamide), and poly(*N*-isopropylacrylamide-*co*-1-vinylimidazole) hydrogel particles. Hydrophobic chains of *N*-octadecylacrylamide were immobilized onto the surface of the poly(*N*-isopropylacrylamide-*co*-1-vinylimidazole) hydrogel particles to use them as anchors for attaching the nanogels onto the lipid bilayers. The diameter of the nanogels prepared varied between 30 and 300 nm. The solvent, temperature, and pH sensitivities of the liposomes, nanogels, and their mixtures were studied. It was found that the phospholipid bilayer always coats the surface of both unanchored and anchored hydrogel particles upon mixing. Aggregation of the lipid bilayer-coated nanogels (lipobeads) was observed when the gel particles collapsed. The mechanism of aggregation differs for the lipobeads containing unanchored cores and those containing anchored hydrogel cores. The hydrogel−liposome structures of a nanometer size are of potential importance for applications such as biomimetic sensory systems, controlled release devices, and multivalent receptors.

Introduction

Artificial systems consisting of only spherical hydrogel particles or liposomes have already found a variety of biomedical applications in drug delivery, drug targeting, protein separation, enzyme immobilization, and so forth.[1−6] Sensory properties of the combined liposome−hydrogel structures reported in this article promise an attractive research field and may lead to novel biomimetic sensory systems.

Liposomes are phospholipid assemblies consisting of a flexible, cell membrane-like lipid bilayer, the surface of which acts as a permeability barrier. Different compounds can be entrapped in the liposome's aqueous interior. It has been shown that liposomes can be constructed with bilayer permeability responsive to a variety of physical and chemical stimuli, including temperature, light, pH, and ions.[7] These liposomes can mimic various functions of biological membranes and can be used as a container for storage, transport, and controllable release of compounds. Furthermore, a liposome can be considered as a nanoscale reactor. Liposomes may be mechanically unstable, and their loading capacity is limited by the water solubility of the material to be loaded,[8] however.

Hydrogel particles are mechanically more stable because of cross-linking and have a greater loading capacity than liposomes do. Their swelling/deswelling properties can be more sensitive to environmental conditions. It has been reported that some polymer gels can swell or shrink discontinuously and reversibly in response to many different stimuli (temperature,[9] pH,[14] ions,[11−14] electric fields,[15] and light[16]), depending on the chemical composition of the gel/solvent system. The volume change can be as large as 1000-fold.[17] Macroscopic gels respond to the environmental changes on a rather long-time scale, however. Tanaka et al.[18] showed that, for a spherical gel, the time required for swelling or shrinking is proportional to the square of its radius. Then, a decrease in the hydrogel size to nanometer scale can solve the problem of slow responses. Hydrogels with faster swelling/deswelling will find more potential applications.

Nevertheless, the hydrogels lack many of useful surface properties of lipid bilayers. Lipid bilayers stabilized on various supports (glass,[25] plastic,[5] metal,[26] and modified polymer[27]) have found a number of applications.[28,29] Bilayer membranes on solid supports are attractive systems mimicking the structural, sensing, and transport roles of biological membranes,[30−34] in particular, sensory systems using ion-channel switches.[32−34] The main drawback of the supported bilayer membranes to date is a lack of well-defined ionic reservoirs on both sides of the membrane. A functional ionic reservoir between a membrane and a substrate can be constructed by using an ion-sensitive hydrogel. In this context, combination of hydrogel particles with liposomes reconstituted with the membrane protein (ionic channel) can be considered as a model system to study the functions of the membrane and membrane proteins and to design new sensory devices. An appropriate assembly of the lipid bilayer on a spherical hydrogel surface can be used to prepare an artificial cell analogue. Furthermore, hydrogel−liposome assemblies combine the properties of both classes of materials, which broaden their potentials for biomimetic sensory systems, controlled release devices, and multivalent receptors.

Preparation and characterization of submicrometer-scale hydrogel particles have intensified recently,[9−14,19−24] but there are few works devoted to fabrication of different combinations of hydrogels and liposomes. A method of fabricating spherical hydrogel particles (beads) within liposomes has been reported[21] in 1997, but this

* Corresponding author: phone 1-718-260 3339, Fax 1-718-260 3125, e-mail klevon@poly.edu.

10.1021/ma011644+ CCC: $22.00
Published on Web 02/01/2002

method required special hydrogel-forming substances with an initiator of gelation that can pass through a liposomal bilayer. Encapsulation of hydrogel particles into liposomes was described by Gao and Huang.[22] Although the overall mechanical strength of the liposomal structure was enhanced in the latter system, the unanchored bilayer was still unstable and needed specific lipid mixtures and polymer cores of certain sizes and shapes. Jin et al.[23] reported design and preparation of a novel hydrogel-anchored lipid vesicle system, called "lipobeads". This system contained (i) a hydrogel polymer core anchored by fatty acids, which were covalently attached to the surface of the hydrogel, and (ii) a lipid layer around the modified hydrogel spherical particle. The bilayer consisting of hydrophobic chains of fatty acids and hydrophobic tails of the phospholipids was more stable than the system described by Gao and Huang.[22] Spherical anionic microgels (6.5 μm at pH 7.0), composed of methylenebis(acrylamide) and methacrylic acid and loaded with doxorubicin, were coated with a lipid bilayer by Kiser et al.[24] to control swelling and release of doxorubicin from the microgels. Yang and coworkers[35] immobilized biotinylated small and large unilamellar liposomes in avidin- or streptavidin-derived gel beads for chromatographic analysis. Recently, the same group[36] reported that egg phosphatidylcholine liposomes and biomembrane fragments could be immobilized on the surface of a poly(acrylamide) macrogel containing hydrophobic anchors, which probably penetrated into the lipid bilayer. Typically, in all works (except one[21]) the sizes of hydrogel particles varied on the micrometer scale, and optical or electron microscopy was used for characterization. This brief review indicates that the research on hydrogel−liposome submicrometer structures is just beginning, and fundamental studies on interactions between hydrogels and liposomes are needed. To the authors' knowledge, dynamic light scattering technique has not been used to measure and characterize different hydrogel/liposome combinations, although the technique gives a detailed account of the state of the suspended nanoparticles.

In the present report, we describe preparation and characterization of hydrogel nanoparticles (nanogels) and liposomes as well as different assemblies of them. The latter hydrogel/liposome system combines complementary advantages of the liposomes and the polymeric hydrogels. Studies of the individual behavior of the hydrogel particles alone and liposomes alone in aqueous solution allowed us to have a better understanding of the behavior of the hydrogel/liposome complex systems.

We prepared the following systems: (i) an unanchored nanogel entrapped in a liposome, (ii) an anchored nanogel entrapped in a liposome, (iii) an aggregate of unanchored nanogels coated with phospholipid bilayer ("giant" lipobeads), and (iv) an aggregate of anchored lipobeads. Unanchored nanogels are based on poly(acrylamide) and poly(*N*-isopropylacrylamide). Anchored nanogels are based on poly(*N*-isopropylacrylamide-*co*-1-vinylimidazole). The dynamic light scattering technique was used to characterize these systems and to measure the size distribution of the hydrogel particles, liposomes, and their assemblies as well as the changes in response to solvent, temperature, pH, and ionic strength variations.

Experimental Section

Materials. Chloroform solution of L-α-phosphatidylcholine from egg yolk (EPC, transition temperature $T_m = -2$ °C, $M_w = 760$ g/mol) was purchased from Avanti Polar Lipids (Alabaster, AL). Acrylamide (AAm), *N*-isopropylacrylamide (NIPA), and 1-vinylimidazole (VI) monomers and *N*,*N*′-methylenebis(acrylamide) (MBA) were purchased from Aldrich (Milwaukee, WI). *N*-(*n*-Octadecyl)acrylamide (ODAm) monomer was obtained from Polysciences (Warrington, PA). 2,2-Diethoxyacetophenone (DEAP) and nonionic detergent Triton X-100 (T_{X-100}) were purchased from Fluka (Milwaukee) and Eastman Kodak (Rochester), respectively. NIPA and AAm were purified by recrystallization from toluene−*n*-hexane (50/50 by volume) and acetone−ethanol (70/30 by volume), respectively, before use. Other chemicals were used directly without further purification. Water purified by Milli-Q (Millipore) at resistivity of 18 MΩ·cm and 50 mM Tris-HCl buffer (pH 7.5) were used in all experiments. 0.1 M HCl or 0.2 M NaOH was used to adjust pH.

Preparation of Liposomes. A conventional procedure[8] to prepare large unilamellar vesicles (LUVs) includes freeze−thaw cycles and extrusion of multilamellar vesicle (MLV) suspension and is time- and labor-consuming. The method leads to a low concentration of liposomes. The procedure of preparing small unilamellar vesicles (SUVs) does not involve freezing and thawing steps, but sedimentation of sonicated MLV suspension results in a much lower concentration of liposomes in the final solution. We avoided extrusion or centrifugation of a MLV suspension but used the probe sonication after freezing and thawing followed by filtration to prevent a loss of the phospholipid and to gain a high yield of monodisperse liposomes.

A needed volume of EPC/chloroform solution with concentration 20 mg/mL of phospholipid was poured into a round-bottom flask. The chloroform was evaporated under flashing with nitrogen to form a lipid film. The film was held under vacuum for at least 3 h and then hydrated by dispersing in 50 mM Tris-HCl (pH 7.5). The volume of the buffer was chosen to provide a final concentration of 5 mg/mL EPC. After gentle handshaking and complete dispersion of lipid, multilamellar vesicles were obtained. Freezing in dry ice/acetone mixture (−77 °C) and thawing (25 °C) was repeated at least five times. Large unilamellar liposomes were prepared by long-time sonication (Ultrasonic Cleaner 50D, VWR Scientific Products) of a milky MLV suspension in a water bath at 20−100 W for 1 h until the sample became transparent. All liposome preparations had a unimodal size distribution within the range of average sizes from 30 to 300 nm. We monitored the average size of liposomes by DLS to find that it does not change for at least 2 days.

Bulky Gel Preparation. Three types of hydrogel [poly(acrylamide) (PAAm), poly(*N*-isopropylacrylamide) (PNIPA), and poly(*N*-isopropylacrylamide-*co*-1-vinylimidazole) (PNIPA−VI)] were prepared by photopolymerization. The procedure of UV-induced polymerization required a photoinitiator within a liquid hydrogel-forming medium entrapped in the liposomal microreactor. A Blak Ray (365 nm, 100 W) mercury lamp was used as a UV light source to initiate polymerization. The temperature (20 °C) was below the lower critical volume phase transition temperatures (T_V) for PNIPA and PNIPA−VI. Polymerization time (τ_P) and macroscopic properties [swelling/deswelling ability, $\alpha = (R/R_0)^3$, R is the radius in a swollen or shrunken state, R_0 is the radius in the prepared state] of the gel depend on the content of monomer/cross-linker mixture, photoinitiator, and light intensity. It is necessary to evaluate the extent of dilution to prevent polymerization and gelation in the solution exterior to liposomes (Table 1, column 7).

To optimize those parameters, bulky (macroscopic) hydrogels of different compositions were synthesized. At high monomer and/or cross-linker concentrations, the swelling/deswelling ability of the gel was small,[9,19] whereas at low concentrations the gel was so soft that two pieces of the gel coalesced and could not be separated upon their contact. (The latter property was important for the preparation of monodisperse nanogels solutions.) Table 1 presents the optimal composition of three types of hydrogel-forming media and properties of the macroscopic hydrogels that were used for nanogels fabrication.

Table 1. Composition of Hydrogel-Forming Media and Properties of Macroscopic Hydrogels Studied

hydrogel	[AAm] (wt %)	[NIPA] (wt %)	[VI] (wt %)	[MBA] (wt %)	[DEAP] (wt %)	dilution (times)	τ_P (h)	sensitivity	α
PAA	4.73			0.47	0.10	20	2	acetone: 40 vol %	∼0.07
PNIPA		5.10		0.51	0.10	20	2	$T_V \sim 32$ °C	∼0.12
PNIPA−VI		5.51	1.97	0.50	0.10	25	2	$T_V \sim 37$ °C	∼0.14
PNIPA−VI		5.51	1.97	0.50	0.10	25	2	pH	∼6

Gelation within Liposomes. In comparison to the already proposed method,[21] our method significantly expands the spectrum of hydrogel-forming components by adding a photoinitiator into the liquid medium inside each liposome and using UV exposure to initiate polymerization and cross-linking within the liposomal microreactor.

Preparation of nanometer-sized hydrogel particles using liposomes as microreactors includes several steps: (i) encapsulation of the hydrogel-forming components into the liposomes, (ii) dilution of LUV suspension to prevent polymerization outside the liposomes, (iii) photopolymerization, (iv) solubilization of the lipid bilayer by detergent (T_{X-100}), (v) removal of the mixed phospholipid−detergent micelles by dialysis, and (vi) drying hydrogel particles by gentle evaporation in a temperature gradient.

To prepare liposomes containing a pregel medium, a mixture of a monomer, a cross-linker, and a photoinitiator (see Table 1) in 50 mM Tris-HCl (pH 7.5) in place of a pure buffer was used at the hydration stage. After freeze−thaw cycles and sonication of MLV solution, the contents of the interior and the exterior of LUV were identical. The LUV suspension was diluted 20−25-fold by the 50 mM Tris-HCl buffer to prevent polymerization in the solution exterior to the liposomes. We did not detect any increase in light scattering intensity of the solution during transition through 32 °C for PNIPA, neither did we for PNIPA-VI at 37 °C, although it is well-known[37] that a concentration of the polymers as low as ∼0.01 mg/mL caused remarkable opalescence during a liquid−liquid phase transition. Further UV exposure[38] of the solution initiated a free radical polymerization, leading to gelation within the liposomal reactor. The hydrogel particle resides within the spherical phospholipid bilayer. To obtain bare hydrogel particles, the phospholipid was removed by adding 15 mM T_{X-100} (critical micelle concentration = 0.15 mM[39]). The mixed phospholipid/detergent micelles thus formed were removed by dialysis in SpectraPore 25 kDa membrane bags against water for 7 days with changing water twice a day. The aqueous solution of the nanogels had a relatively low level of light scattering intensity because of a low refractive index difference with water. The concentration of the hydrogel nanoparticles was increased by evaporation of water in a temperature gradient (from +30 to −77 °C) under vacuum and flashing with nitrogen. Dried hydrogel particles were dissolved in a needed volume of water or buffer. After redispersion in aqueous medium by sonication, the same average size of the hydrogel particles as the one before drying was restored, as evidenced in the DLS measurements. The concentration of the nanogels was below 1 mg/mL, and we did not see concentration dependence of the size distribution in this range. Solutions of hydrogel particles of different polymer types were used for mixing with liposomes and DLS characterization of those mixtures.

Hydrophobic Modification of the Surface of Hydrogel Particles. In general, hydrophobic compounds with a long hydrocarbon tail cannot be introduced directly into the liposome because they are insolubile in water. To introduce an insoluble but reactive component into the liposome, we added an anchoring monomer into the phospholipid/chloroform solution at the step of MLV formation. After preparation of unilamellar liposomes, hydrophobic anchors were apparently incorporated into the lipid bilayer.

The procedure to prepare hydrogel particles with hydrophobic anchors attached to the surface was essentially the same as the preparation of unanchored nanogels except that ODAm was dissolved in the initial phospholipid/chloroform solution. The amount of the added ODAm was in the molar ratio of phospholipid to ODAm equal to 70:1. This ratio provides the maximal loading capacity of lipid bilayer.[40−43] Hydrophobic ODAm monomers were incorporated into the lipid bilayer on the step of dry lipid film formation. After LUV formation, free ODAm (insoluble in water) is removed by filtration through a 0.45 μm filter. During UV exposure, the PNIPA-VI-*co*-ODAm copolymer was assumed to form the following structure:

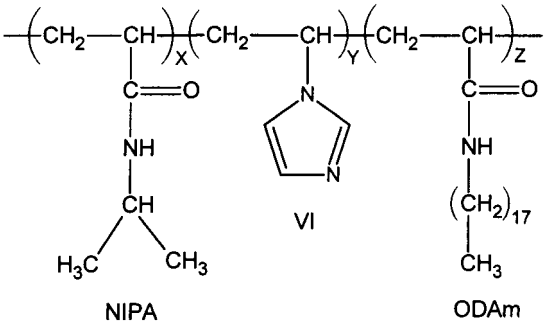

The other steps of preparation were the same as those for the preparation of unanchored hydrogel particles.

The interaction between nanogels and liposomes and behavior of different hydrogel/liposome structures were studied when the liposome suspension was added into the vials with the solution of unanchored or anchored hydrogel particles. We evaluated the number of particles in unit volume from the weight concentration of the solution and the diameter of the particle. The number of phospholipid molecules in liposome of a given size[43] was also used to estimate the number of liposomes in unit volume. The mixtures were incubated for 2 h at room temperature with gentle shaking.

Dynamic Light Scattering Analysis. Dynamic light scattering (DLS) measurements were done with a N4 Plus particle size analyzer (Coulter Electronics, Hialeah, FL). A He−Ne laser operating at 628 nm wavelength and 10 mW output power was used as a light source. The scattering angle was held constant at 90°. The temperature was controlled within ±0.1 °C from the set temperature. Solutions were filtered into a square glass cuvette (10 mm) using a 0.45 μm Millipore Millex filter. The quality of measurements was checked over the apparent signal-to-noise ratio of the autocorrelation function, the overflow count, and the baseline error. When the field−field correlation function was close to single exponential, the cumulant analysis was used. The particle size distribution and the average particle diameter, $\langle d \rangle$, were obtained from the correlation function by CONTIN analysis using standard software supplied by Coulter Electronics.

Results and Discussion

Liposomes. The size distribution curves for pure (or solvent-filled) EPC liposomes were obtained. The curve for the 11 times extruded liposomes (Figure 1a) exhibited a wide unimodal distribution with a peak at 161 nm. We found that this method of liposome preparation was time-consuming, and a large amount of phospholipid was lost during the extrusion. In general, the curves for 1 h sonicated liposomes (Figure 1b,c) exhibited a narrower unimodal distribution. The *z*-average hydrodynamic diameter $\langle d \rangle$ depends on the power of the sonifier. The width of the distribution could be governed by the duration of sonification. Thus, one can control

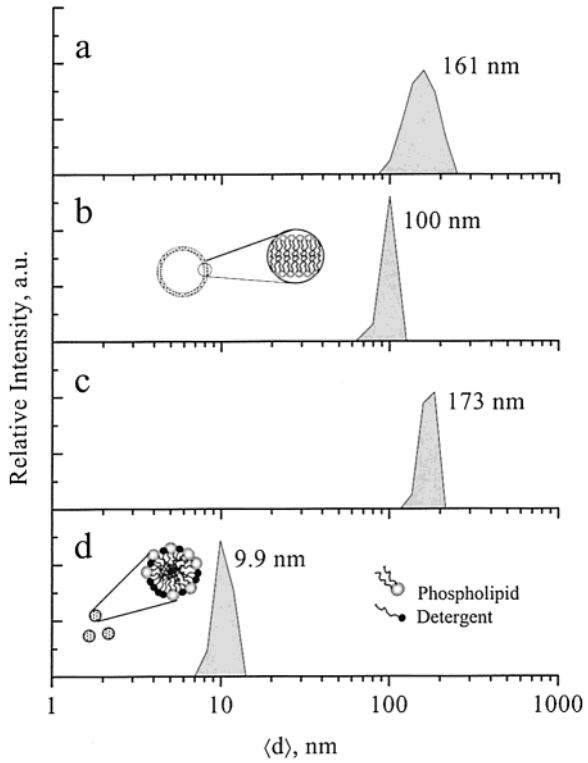

Figure 1. Size distribution curves for liposomes in 50 mM Tris-HCl buffer: (a) prepared by extrusion through two stacked polycarbonate membranes with 100 nm pores (11 times); (b) prepared by sonication with the sonifier power of 60 W; (c) prepared by sonication with the sonifier power of 20 W; (d) mixed T_{X-100}−EPC micelles.

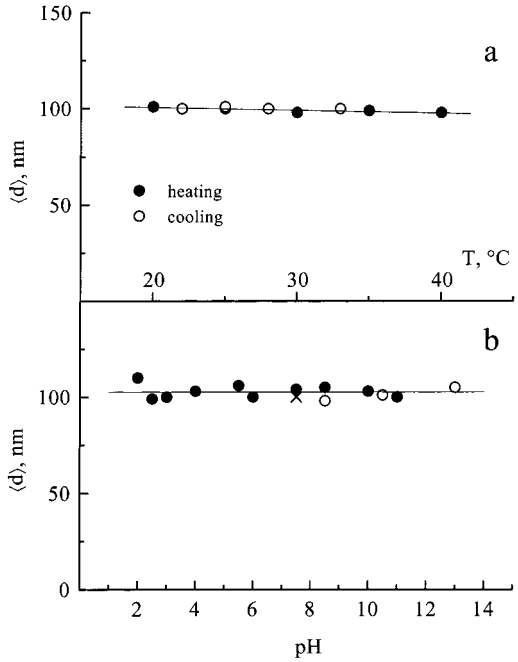

Figure 2. (a) *z*-Average diameter of the liposomes as a function of temperature during heating/cooling cycles. The linear regression fit is shown by a line. (b) pH dependence of the average diameter of the liposomes prepared at pH 7.5 (×); pH was increased by adding 0.2 M NaOH (open circles); pH was decreased by adding 0.1 M HCl (solid circles). The solid line indicates the average diameter over the entire pH range.

the size distribution of the liposomes and also the hydrogel particles prepared within liposomes. The size distribution curves for liposomes sonicated at different powers are compared in Figure 1b,c. At the conditions mentioned earlier (see Preparation of Liposomes), the liposomes with an average diameter between 30 and 300 nm were reliably detected. We observed that our method, without loss of phospholipid, provides a higher concentration of liposomes and therefore a higher concentration of hydrogel particles.

A liposome can be destroyed by solubilization of the phospholipid bilayer. Detergents are widely used for this purpose:[39,44] the micelle-forming amphiphiles compete with the bilayer lipids to dissolve the bilayer into the amphiphile micelles. At low detergent/lipid ratios, each detergent molecule adsorbs onto the bilayers.[39] With an increasing detergent/lipid ratio, the amount of the detergent on the bilayer increases until the detergent breaks up the bilayer into many lipid−detergent micelles. A further increase in the detergent/lipid ratio leads to delipidation of the lipid−detergent mixed micelles. We added 15−50 mM of T_{X-100} into the solution of liposomes. Figure 1d shows that the addition of the detergent results in disappearance of the peak at 100 nm and appearance of a new peak at 9.9 nm. Lopez et al.[39] showed that the size distribution curves for micellar T_{X-100} solutions presented a unimodal distribution with a peak at 9 nm, whereas for the mixture of 2 mM T_{X-100} and liposomes they obtained the average diameter at around 17 nm. Our intermediate micellar diameter indicates that the size of mixed micelles increases with an increase in the concentration of the phospholipids.

Figure 2a presents the temperature dependence of the average diameter $\langle d \rangle$ of EPC liposomes between 20 and 40 °C. In the temperature range above the main transition temperature (−2 °C), there was a slight decrease in $\langle d \rangle$ with an increasing temperature. The decrease was less than 5% in the range studied. There was almost no difference in $\langle d \rangle$ between the heating (solid circles) and cooling (open circles) scans, indicating a reversible change without thermal hysteresis.

Figure 2b shows the pH independence of $\langle d \rangle$ of EPC liposomes at 25 °C. EPC is a neutral phospholipid, and therefore one cannot expect pH-responsive fusion of the lipid bilayer.[45−47] As a matter of fact, we found a tendency of liposomes to aggregate at low pH (pH < 3), a result ascribed to possible protonation and neutralization of the P^--N^+ dipole in phosphocholine on the liposome interface and/or to destruction of the hydration shell[48] consisting of interfacial water molecules in close contact with lipid polar headgroups.

Solvent-Sensitive PAAm Hydrogel Particles. PAAm nanogels covered with phospholipid bilayers (lipobeads) have been prepared by photopolymerization using liposomal microreactors. A typical particle size distribution and structure of the lipobeads obtained after UV-induced polymerization are displayed in Figure 3a. A unimodal, but relatively broad, size distribution was obtained. After addition of 15 mM T_{X-100} and 5−10 min mixing, a peak for large particles (∼200 nm) and a peak for small particles (∼9 nm) were detected (Figure 3b). The total scattering intensity decreased to less than one-tenth. Thus, addition of T_{X-100} resulted in solubilization of the phospholipid bilayer. The smaller particles are ascribed to the mixed micelles depicted in Figure 3b. To identify the larger particles as pure PAAm hydrogel particles, an ability of the hydrogel to swell or shrink in response to environmental changes can be

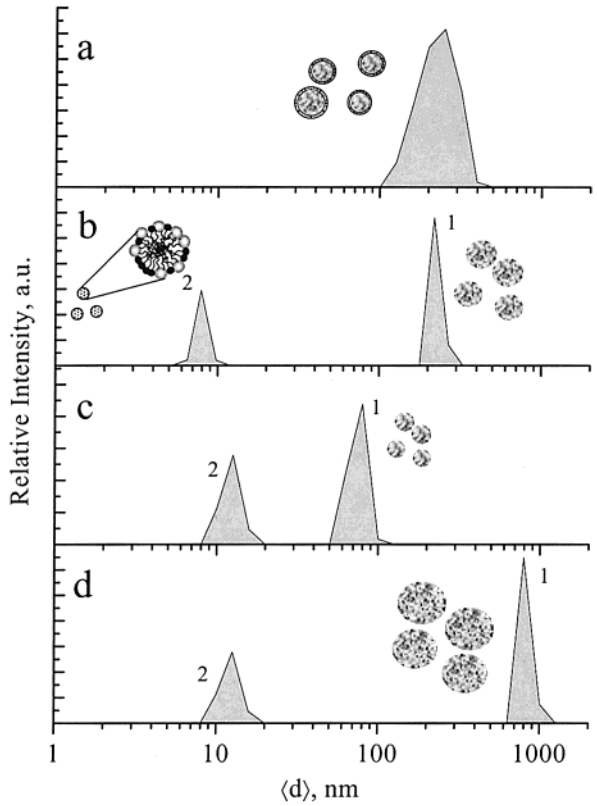

Figure 3. Size distribution curves for (a) PAAm lipobeads in buffer and (b) after addition of 15 mM T_{X-100}. The effect of (c) 40 vol % and (d) 10 vol % acetone. 1, PAAm hydrogel particles; 2, mixed T_{X-100}−EPC micelles.

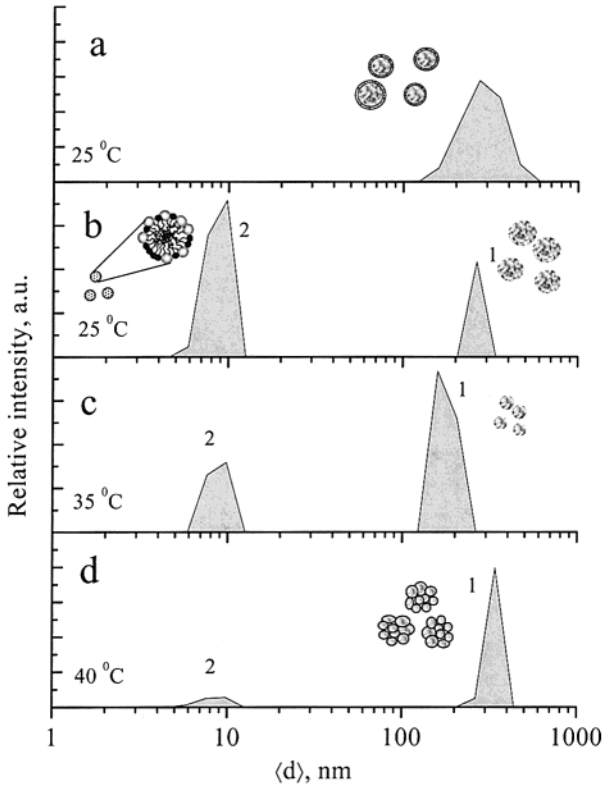

Figure 4. Size distribution curves for (a) PNIPA lipobeads in buffer at 25 °C, (b) after addition of 15 mM T_{X-100} at 25 °C, (c) at 35 °C, and (d) at 40 °C.

exploited. Poly(acrylamide) gels are not temperature- or pH-sensitive, but it has been observed[49] that PAAm gels in water−acetone mixtures swell or collapse as a function of the acetone concentration. In particular, it has been shown[50] that the gel is swollen at concentrations less than 37 vol % of acetone; otherwise, the gel is collapsed. Two concentrations of acetone were selected to confirm that solvent-sensitive hydrogel particles were obtained. At 40 vol % of acetone a shift of the 200 nm peak to a smaller size ($\alpha \approx 0.045$) was observed (Figure 3c). At 10 vol % of acetone, however, a volume of the PAAm nanogels was increased by a factor 45 as seen in Figure 3d.

The observed volume changes of our hydrogel particles are much greater compared with PAAm macrogels.[50] It is known that the swelling ratio of macrogels changes over a long time to approach some equilibrium value (aging phenomenon). We consider that the nanometer-size hydrogel particles can reach the maximal capability of swelling/deswelling within our observation time scales.

In parts c and d of Figure 3, mixed detergent/phospholipid micelles increase their size from 9 to 12 nm after addition of acetone. It may be a result of penetration of less polar acetone molecules into the nonpolar interior of micelles, leading to formation of microemulsions.

Temperature-Sensitive PNIPA Hydrogel Particles. Figure 4a shows that a relatively broad size distribution of PNIPA lipobeads with a peak at around 250 nm was obtained at 25 °C after UV exposure of a diluted LUV suspension containing initial components of PNIPA gels (see Table 1, row 3). It is essential to confirm the formation of hydrogel within each liposome. Figure 4b demonstrates that adding T_{X-100} in a molar ratio of 45:1 (detergent/lipid) resulted in two peaks with maxima at (1) 250 nm and (2) 9 nm, ascribed to the PNIPA hydrogel particles and the mixed detergent−phospholipid micelles, respectively. The ratio of the scattering intensities of small and large particles indicates that the concentration of the nanogels is relatively low.

PNIPA gels exhibit a volume phase transition temperature at T_V. We increased the temperature above the volume phase transition temperature $T_V \sim 32$ °C. We expected shrinking of the PNIPA hydrogel particles. Interestingly, at 35 °C (Figure 4c) the peak position for the larger particles shifted toward a smaller size whereas at 40 °C (Figure 4d) the peak moved to a larger size. During these changes from 25 to 40 °C, the absolute intensity of the light scattered from the small particles (2) did not change, but the absolute scattering intensity of the larger particles progressively increased upon elevating the temperature. The latter behavior can be explained only if the PNIPA hydrogel particles shrink up to 35 °C and the shrunken particles aggregate at 40 °C.

When we removed the solubilized phospholipid and detergent molecules as well as mixed micelles by dialysis against water and concentrated this suspension by evaporation in temperature gradient, the average diameter of pure PNIPA nanogels was found to be around 200 nm at 25 °C (Figure 5a). At 35 °C (above T_V) the size distribution (Figure 5b) shows two peaks. If the peak at ∼98 nm is the average diameter of the shrunken beads, the swelling ratio α is around 0.13. The peak for the larger particles at ∼398 nm should represent aggregates of collapsed hydrogel particles.

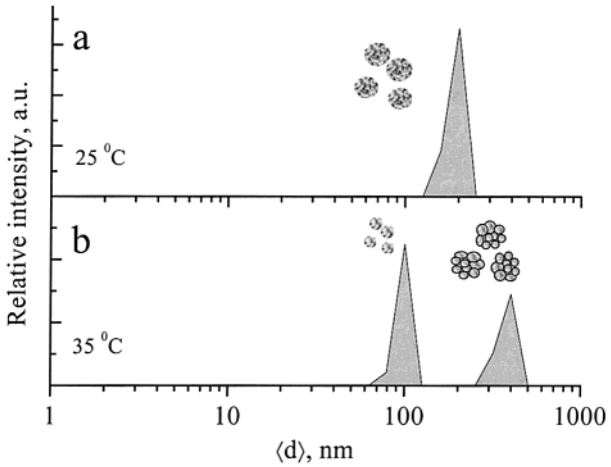

Figure 5. Size distribution curves for the pure PNIPA hydrogel particles in water (a) below and (b) above the volume phase transition temperature.

It is worthwhile to note that, despite aggregation, the solution remains stable and transparent, indicating that the aggregates are still colloidally stable at least in the time scale of interest. Colloid stability depends on the balance of the van der Waals attraction and the electrostatic repulsion. Below T_V, PNIPA nanogels are colloidally stable because the gel matrix is hydrated, and therefore the van der Waals attractive forces between particles are relatively small. Electrostatic repulsion is also small, as was indicated by the low electrophoretic mobility of PNIPA microgel.[51] Above T_V, the water content of the gels is reduced, giving a higher matrix density and greater attractive forces between the hydrogel particles. At elevated temperatures, the PNIPA microgels are stable only at low electrolyte concentrations. At low ionic strengths, the electrophoretic mobility of PNIPA microgels is high,[51] indicating that electrostatic stabilization can take place. Furthermore, disruption of the hydrodynamic shell around the gel particles with an increasing temperature will promote aggregation as well. It seems reasonable to assume that the surface of the shrunken PNIPA hydrogel particles is more hydrophobic than the swollen ones. Aggregation will reduce the total hydrophobicity by decreasing the total surface of the particles. The fine balance of the van der Waals forces and the electrostatic forces determines the resultant size of the aggregates. If both forces are weak, large fluctuations of the aggregate size can occur.

Mixture of Pure PNIPA Nanogels and Liposomes. Figure 6a,b shows the size distribution curves at 25 °C for liposomes and pure PNIPA nanogels before mixing with approximately the same average diameter of ca. 180 nm. Then we added liposomes into the suspension of pure PNIPA nanogels so that the evaluated ratio of particles was 1:1. If both particles existed independently without interactions, one could expect that upon increasing temperature the hydrogel particles would shrink, whereas liposomes would not change the size, and two separate peaks would be detected; if both particles formed aggregates, resultant particles at least twice the size should be observed, as we have seen in Figures 4 and 5. On the other hand, one can expect that the temperature dependence of the bare PNIPA nanogels and the nanogels covered by lipid bilayer (lipobeads) has to be different. In accord with the results of the previous section, PNIPA nanogels collapse and aggregate above T_V. Lipobeads should not change size due to the temperature independency of the pure liposomes (see Figure 2).

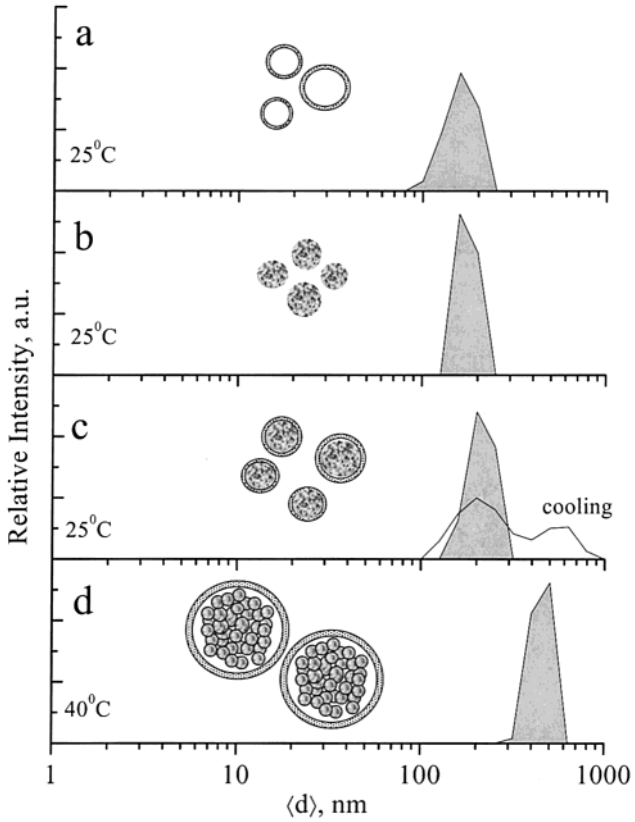

Figure 6. Size distribution curves for (a) liposomes, (b) pure PNIPA nanogels, and their mixture (c) below and (d) above the volume phase transition temperature. The line in (c) gives the distribution upon cooling from 40 °C.

In fact, at 25 °C we found only a single peak (Figure 6c) with the average diameter slightly greater than the diameter of the liposomes and the PNIPA nanogels before mixing. When the temperature was raised to 40 °C (above T_V), the single peak significantly shifted toward a larger diameter (Figure 6d). In bare PNIPA nanogels, in contrast, the peak for isolated particles shifted to a smaller diameter, and the second peak for aggregates appeared at a larger diameter, when heated (Figure 5). The presence of one peak only and the increase in the particle size in the hydrogel particles/liposomes mixture can be explained only by assuming that during the mixing a phospholipid bilayer of the liposomes covers each PNIPA nanogel, resulting in a lipobead, as illustrated in Figure 6c. Apparently, this configuration must be energetically more preferable over the others. Note that considerable hydrophobicity of the PNIPA gel might be hidden within the liposome. The same discussion can explain fusion of lipobeads and aggregation of collapsed hydrogel particles at elevated temperatures. The collapse of the hydrogel particles at 40 °C yields the "giant" lipobeads with a structure depicted in Figure 6d.

This pattern of nanogels aggregation and giant lipobeads formation appears to be irreversible or have a thermal hysteresis. Figure 6c shows the size distribution of the liposome−nanogel mixture after cooling to 25 °C and temperature equilibration for 2 h. The presence of two peaks indicates that some giant lipobeads did not break up into elementary lipobeads.

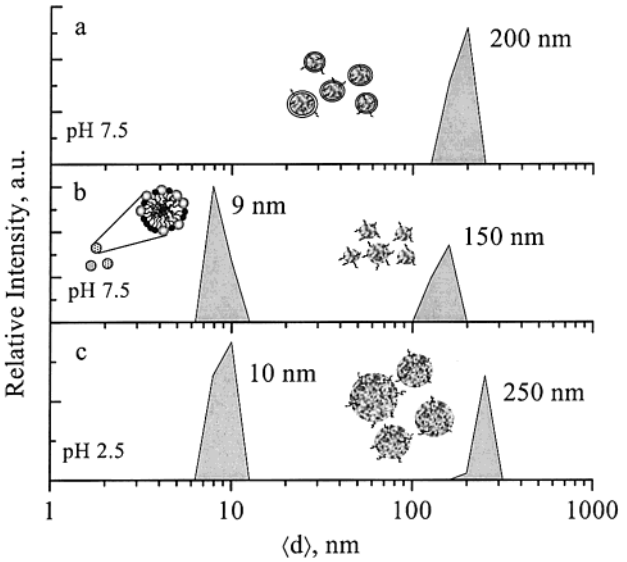

Figure 7. Size distribution curves for (a) PNIPA−VI lipobeads in buffer (pH 7.5), (b) after addition of 15 mM T_{X-100}, and (c) at pH 2.5.

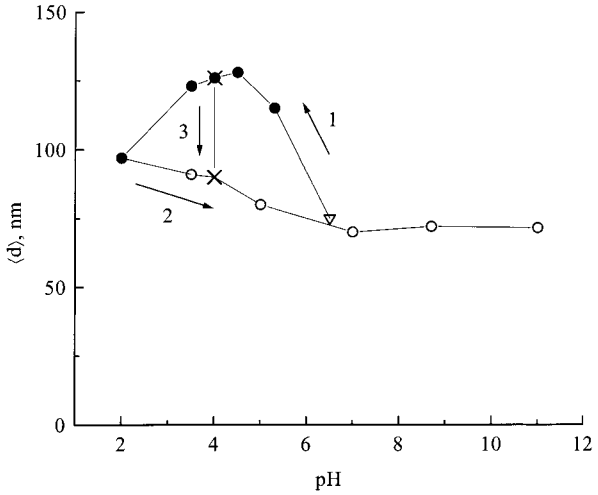

Figure 8. pH Dependence of the average diameter of the pure PNIPA−VI nanobeads. First, pH was decreased by addition of 0.1 M HCl (solid circles, arrow 1). Then, pH was increased by addition of 0.2 M NaOH (open circles, arrow 2). Change of the nanogels size after addition of 10 mM NaCl at pH 4.0 is shown by arrow 3.

Temperature- and pH-Sensitive PNIPA−VI Hydrogel Particles. It is of our interest to prepare hydrogel particles which would combine thermo-, pH-, and ionic sensitivities with capability of binding to the surface of phospholipid bilayer. It has been already shown that T_V and the swelling ability can change dramatically for submicrometer gel beads based on PNIPA when ionizable groups are incorporated within the polymer network.[57] One of the recent synthetic techniques to prepare PNIPA-based spherical gel particles is aqueous redox polymerization in different media[9] such as surfactant-containing water, surfactant-free water, and water suspended in oil.

There is a number of methods to incorporate the ionizable groups into the gel network: (i) covalent binding of ionizable groups in the initiator to the end groups of the PNIPA chains during polymerization;[53,54] (ii) aqueous redox copolymerization of NIPA with ionic monomers (e.g., methacrylic acid,[55] *N*-(acryloxy)succinimide,[56] acrylic acid,[57] 1-vinylimidazole (VI),[57] and combination of acrylic acid and 1-vinylimidazole[58]).

The present section reports preparation and characterization of anchored hydrogel particles composed of PNIPA network into which a cationic monomer, VI, was incorporated by UV-induced polymerization within liposomal microreactors (Table 1, row 3). Preparation of nanogels in liposomes is reasonable regarding not only the size distribution reproducibility but also a possibility to immobilize the hydrophobic anchors onto the surface of the particles. We introduced water-insoluble *N*-octadecylacrylamide (ODAm) into the liposomal membrane in the step of dry phospholipid film formation. After the liposome formation, hydrophobic residues penetrate into lipid bilayer, whereas hydrophilic heads of ODAm covalently bind to the polar end groups of the PNIPA−VI chains on the surface of the network during UV copolymerization. As a result, anchored PNIPA−VI lipobeads with the diameter of around 200 nm were synthesized (Figure 7a).

The fabrication of hydrogel particles was confirmed by removing the vesicle phospholipid bilayer from the lipobeads using detergent (T_{X-100}). As shown in Figure 7b, two peaks corresponding to the mixed detergent/lipid micelles (∼9 nm) and the PNIPA-VI nanogels (∼150 nm) were observed at pH 7.5 and 25 °C. To answer the question, whether the ionizable VI monomers actually were incorporated into the PNIPA network, the pH was reduced to 2.5. The acidic environment should result in formation of $\equiv NH^+Cl^-$ groups in the gel particles. Figure 7c shows that the size of the PNIPA−VI hydrogel particles at pH 2.5 increased (∼250 nm) compared with the size of the gel particles that have $=N-$ groups at pH 7.5. The estimated swelling ratio of $\alpha \approx 4.6$ demonstrates the pH sensitivity of the prepared PNIPA−VI nanogels.

A more detailed study of the swelling/deswelling of the nanogels with pH change was performed when the phospholipid and detergent molecules were removed by dialysis against water (pH 6.5), followed by concentration due to evaporation.

The pH dependence of the diameter for the pure PNIPA−VI nanogels (Figure 8) demonstrates that the diameter $\langle d \rangle$ increased from 75 nm at pH 6.5 to 128 nm at pH 4.5 (arrow 1) when the neutral imidazolyl groups were converted into the protonated form. The swelling resulted from imbalance between repulsive electrostatic forces (ionic osmotic pressure) and attractive forces of the polymer network (network swelling pressure). When the pH decreases from 7 to 4.5, the concentrations of acidic ions (H^+ and Cl^-) will increase with decreasing pH in the solution surrounding. Those ions will be attracted into the gel and be involved in the protonation of the imidazolyl groups. Until all imidazole groups are protonated, a decrease in pH will increase the ion swelling pressure. To compensate it, the polymer network must swell. Eventually, all imidazolyl groups will be converted into the saline form according to equation

$$=N- \xrightarrow{HCl} \equiv NH^+Cl^-$$

All imidazolyl groups are ionized at pH 4.5. A further decrease in pH will cause excess acidic ions (H^+ and Cl^-) in the gel and screening of the ionizable groups.[52,55,59] The latter phenomenon results in a drop of the ion swelling pressure. Again, to compensate the decrease, the gel shrinks. We observed a contraction in the range of pH from 4.5 to 2. It is interesting to note that a

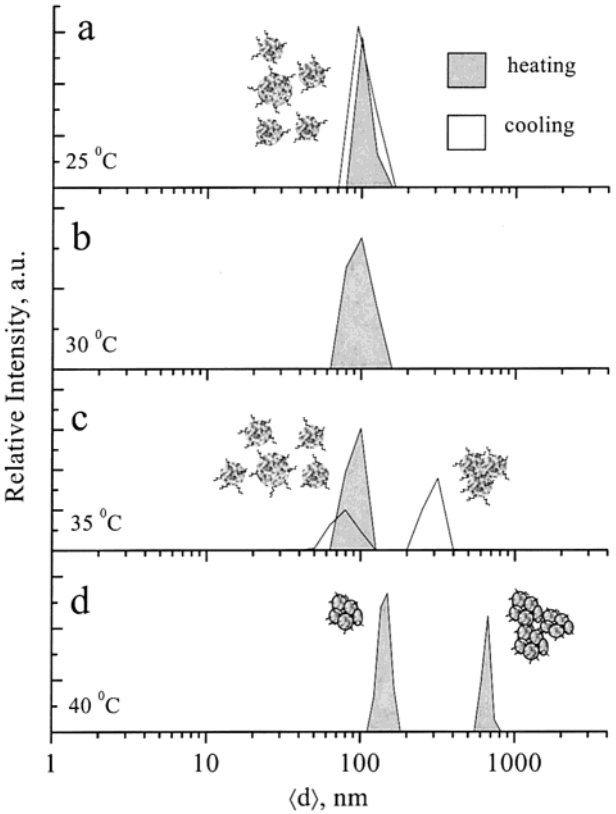

Figure 9. Effect of temperature on the collapse and subsequent aggregation of PNIPA−VI nanogels. The size distribution curves for pure PNIPA−VI nanogels in water (a−c) below and (d) above the volume phase transition temperature. The solid lines in (c) and (a) give the distribution upon cooling from 40 °C to 35 °C and 25 °C, respectively.

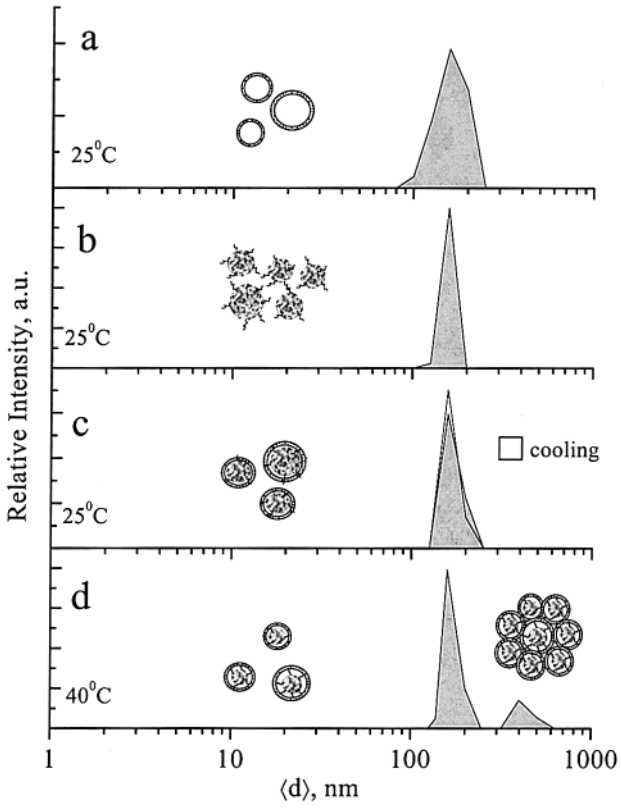

Figure 10. Size distribution curves for (a) liposomes, (b) anchored PNIPA−VI nanogels, and their mixture (c) below and (d) above the volume phase transition temperature. The solid line in (c) gives the distribution upon cooling from 40 °C.

subsequent increase in pH (arrow 2) by adding NaOH only resulted in a substitution of excess hydrogen counterions H^+ for sodium counterions Na^+, so that the screening of the charged species intensified. The physical dimensions of the gels did not return to the maximal size but continued to decrease until neutral. This process is analogous to the addition of NaCl when all ionizable groups of imidazole are protonated. The arrow 3 in Figure 8 shows the corresponding change in the diameter of the nanogels upon adding 10 mM NaCl into the gel suspension at pH 4.0. A further increase in pH by additing NaOH (arrow 2) restored the size of the hydrogel particles to minimize at pH 7.0. No significant change in size was observed in the range of pH from 7 to 11; most imidazolyl groups were already deprotonated. Thus, the data shown in Figure 8 confirm the pH and ionic sensitivities of the PNIPA−VI nanogels at pH from 7 to 2. At pH ≥ 6.5 where the ionic and pH sensitivities are weak, the changes of the nanogels size were detected at around the temperature of volume phase transition of the polymer, as shown below.

Figure 9a−c shows that $\langle d \rangle$ of anchored PNIPA−VI hydrogel particles remains almost unchanged between 25 and 35 °C at pH 6.5. Above $T_V \approx 37$ °C, we expect that contraction of the nanogels increases their hydrophobicity, leading to aggregation. The data for 40 °C shown in Figures 9d are in agreement with this expectation. At elevated temperatures, extensive aggregation of collapsed nanogels results in a bimodal distribution with peaks at larger values of $\langle d \rangle$ compared with those below T_V. A further rise in the temperature increased the light scattering intensity sharply. Turbidity of the suspension was so strong that light scattering measurements were impossible. The aggregation of anchored nanogels was confirmed by the fact of its partial irreversibility upon cooling to 35 °C (see Figure 9c). Probably, restoring the initial particles size requires a longer time under cooling compared with heating. (In our experiment, the equilibration time was ∼30 min after the temperature change.) Nevertheless, after cooling to 25 °C the size distribution curve for the anchored PNIPA−VI nanogels was restored (Figure 9a).

PNIPA−VI Lipobeads. Figure 10a,b shows the size distribution curves for liposomes and pure anchored PNIPA−VI nanogels with again (see Figure 6) approximately close average diameters of ca. 160 nm. The mixture of the liposomes and the anchored nanogels in approximately 1:1 number ratio had the size distribution curve shown in Figure 10c. Comparison of these three curves leads to a conclusion that the size distribution curve for the mixture is determined by the size distribution of the nanogels. Following the discussion for the mixture of unanchored PNIPA nanogels and liposomes, one might come to a conclusion that each anchored PNIPA−VI hydrogel particle is coated with a phospholipid bilayer, forming a lipobead, as seen in Figure 10c.

In contrast to PNIPA lipobeads, the anchored PNIPA−VI lipobeads did not change the average size during volume phase transition (the large peak in Figure 10d). Moreover, the only 3% increase in the total scattering intensity indicates that only a few anchored lipobeads aggregated at elevated temperatures. After cooling (Figure 10c), the size of the anchored lipobeads was entirely restored and the aggregates dissolved. The observed reversibility of the swelling/deswelling behav-

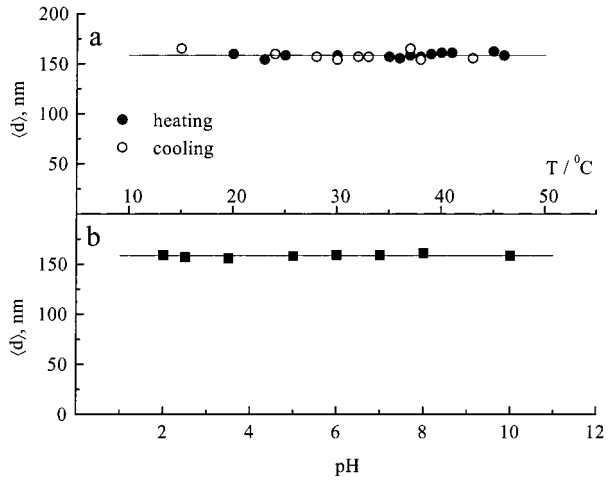

Figure 11. *z*-Average diameter of the anchored PNIPA−VI lipobeads (a) as a function of temperature upon heating/cooling and (b) as a function of pH.

ior indicates that the anchored lipobeads aggregate without fusion. They touch each other but do not form a "giant" lipobead. Obviously, the aggregates of anchored lipobeads shown in Figure 10d disassemble more easily than the "giant" lipobeads do.

We also found that the anchored PNIPA−VI lipobeads have a high stability against temperature and pH changes as shown in Figure 11, a and b, respectively. It is likely that PNIPA−VI nanogels may go through a shrinking at $T_V \sim 37$ °C (Figure 9) or may exhibit swelling/deswelling from pH 7 to pH 2 (Figure 8), but being within the interior of liposomes, the changes of the gel size are hidden by the temperature and pH stabilities of the lipid bilayer. There may be another reason for the pH independence of anchored lipobeads: The hydrophobic chains of the anchors penetrate the bilayer, which manifests itself as a barrier to the pH changes. Then pH may be different between outside and inside the liposome. This stabilizing effect remains to be proven.

Conclusions

We established a protocol to prepare hydrogel particles of various chemistries with a uniform diameter between 30 and 300 nm in the swollen state by using a liposome microreactor. Dynamic light scattering was used to measure the size distribution of nanogels and their complexes with liposomes that coat the gel surface. The changes in size and the aggregation state upon temperature and pH changes were also studied.

In one type of nanogels we demonstrated that the mechanical stability and chemical impermeability of the phospholipid bilayer could be improved by its hydrophobic anchoring. It will be important for studying the interaction between protein incorporated into the liposomal membrane as an ionic channel and the hydrogel as an ionic reservoir. This possibility will be also useful for designing controlled release devices.

Our methods for fabrication and functionalization of nanogels and lipobeads and the obtained particles themselves thus prepared may have numerous promising applications in supramolecular chemistry, nanobiotechnology, medicine, and pharmaceutical industry. One can consider, for instance, applications of the hydrogel−liposome systems as biomimetic sensory systems, controlled release devices, and multivalent receptors.

Acknowledgment. Financial support from DARPA (Grant 0660076225) is gratefully acknowledged.

References and Notes

(1) Rolland, A. *Pharmaceutical Particulate Carriers: Therapeutic Applications;* Dekker: New York, 1993.
(2) Rogers, J. A.; Choi, Y. W. *Pharm. Res.* **1993**, *10*, 913.
(3) Ong, S.; Liu, H.; Qiu, X.; Bhat, G.; Pidgeon, C. *Anal. Chem.* **1995**, *67*, 755.
(4) Cai, S. J.; McAndrew, C. S.; Leonard, B. P.; Chapman, K. D.; Pidgeon, C. *J. Chromatogr. A* **1995**, *696*, 49.
(5) Rothe, U.; Aurich, H.; Engelhard, H.; Desterhelt, D. *FEBS Lett.* **1990**, *263*, 308.
(6) Chang, T. M. S. *Artif. Cells Immob. Biotechnol.* **1992**, *20*, 159.
(7) Gerasimov, O. V.; Rui, Y.; Thompson, D. H. In *Vesicles*; Rosoff, M., Ed.; Marcel Dekker: New York, 1996; p 679.
(8) Gregoriadis, G. *Liposome Technology*, 2nd ed.; CRC Press: Boca Raton, FL, 1994; Vol. III.
(9) Pelton, R. *Adv. Colloid Interface Sci.* **2000**, *85*, 1 and references therein.
(10) Tanaka, T.; Fillmore, D.; Sun, S. T.; Nishio, I.; Swislow, G.; Shah, A. *Phys. Rev. Lett.* **1980**, *45*, 1636.
(11) Eichenbaum, G. M.; Kiser, P. F.; Simon, S. A.; Needham, D. *Macromolecules* **1998**, *31*, 5084.
(12) Eichenbaum, G. M.; Kiser, P. F.; Dobrynin, A. V.; Simon, S. A.; Needham, D. *Macromolecules* **1999**, *32*, 4867.
(13) Eichenbaum, G. M.; Kiser, P. F.; Shan, D.; Simon, S. A.; Needham, D. *Macromolecules* **1999**, *32*, 8996.
(14) Markland, P.; Zhang, Y.; Amidon, G. L.; Yang, V. C. *J. Biomed. Mater. Res.* **1999**, *47*, 595.
(15) Tanaka, T.; Nishio, I.; Sun, S. T.; Nishio, S. U. *Science* **1982**, *218*, 467.
(16) Suzuki, B.; Tanaka, T. *Nature (London)* **1990**, *346*, 345.
(17) Erman, B.; Flory, P. J. *Macromolecules* **1986**, *19*, 2342.
(18) Tanaka, T.; Fillmore D. J. *J. Chem. Phys.* **1979**, *70*, 1214.
(19) Wu, C. *Polymer* **1998**, *39*, 4609 and references therein.
(20) Kratz, K.; Hellweg, T.; Eimer, W. *Polymer* **2001**, *42*, 6631.
(21) Monshipouri, M.; Rudolph, A. S. U.S. Patent No. 5626870, 1997.
(22) Gao, K.; Huang, L. *Biochim. Biophys. Acta* **1987**, *897*, 377.
(23) Jin, T.; Pennefather, P.; Lee, P. I. *FEBS Lett.* **1996**, *397*, 70.
(24) Kiser, P. F.; Wilson, G.; Needham, D. *Nature (London)* **1998**, *394*, 459.
(25) Bayer, T. M.; Bloom, M. *Biophys. J.* **1990**, *58*, 357.
(26) Plant, A. L. *Langmuir* **1993**, *9*, 2764.
(27) Spinke, J.; Yang, J.; Wolf, H.; Liley, M.; Ringsdorf, H.; Knoll, W. *Biophys. J.* **1992**, *63*, 1667.
(28) (a) Sackman, E. *Science* **1996**, *271*, 43. (b) Sackman, E.; Tanaka, M. *TIBTECH* **2000**, *18*, 58.
(29) McConnell, H. M.; Watts, T. H.; Weis, R. M.; Brian, A. A. *Biochim. Biophys. Acta* **1986**, *864*, 95.
(30) Woodhouse, G. E.; King, L. G.; Wieczorek, L.; Cornell B. A. *Faraday Discuss.* **1998**, *111*, 247.
(31) Wagner, M. L.; Tamm, L. K. *Biophys. J.* **2000**, *79*, 1400.
(32) Raguse, B.; Braach-Maksvytis, V.; Cornell, B. A.; King, L. G.; Osman, P. D. J.; Pace, R. J.; Wieczorek, L. *Langmuir* **1998**, *14*, 648.
(33) Cornell, B. A.; Braach-Maksvytis, V.; King, L. G.; Osman, P. D. J.; Raguse, B.; Wieczorek, L.; Pace, R. J. *Nature (London)* **1997**, *387*, 580.
(34) Kasianowicz, J. J.; Henrickson, S. E.; Weetall, H. H.; Robertson, B. *Anal. Chem.* **2001**, *73*, 2268.
(35) Yang, Q.; Liu, X.; Ajiki, S.; Hara, M.; Lundahl, P.; Miyake, J. *J. Chromatogr. B* **1998**, *707*, 131.
(36) Hara, M.; Yuan, H.; Miyake, M.; Iijima, S.; Yang, Q.; Miyake, J. *Mater. Sci. Eng. C* **2000**, *13*, 117.
(37) Kazakov, S. V.; Galaev, I. Yu.; Mattiasson, B. *Int. J. Thermophys.*, in press. Paper presented at 14th Symposium on Thermophysical Properties, June 25−30, 2000, Boulder, CO.
(38) Reiser, A. *Photoreactive Polymers. The Science and Technology of Resists*; John Wiley & Sons: New York, 1989.
(39) Lopez, O.; Cocera, M.; Pons, R.; Azemar, N.; Lopez-Iglesias, C.; Wehrli, E.; Parra, J. L.; de la Maza, A. *Langmuir* **1999**, *15*, 4678.
(40) Zignati, M.; Drummond, D. C.; Meyer, O.; Hong, K.; Leroux, J.-Ch. *Biochim. Biophys. Acta* **2000**, *1463*, 383.
(41) Ringsdorf, H.; Venzmer, J.; Winnik, F. M. *Angew. Chem., Int. Ed. Engl.* **1991**, *30*, 315.
(42) Watts, A.; Marsh, D.; Knowles, P. F. *Biochemistry* **1978**, *17*, 1792.
(43) Huang, C.; Mason, J. T. *Proc. Natl. Acad. Sci. U.S.A.* **1978**, *75*, 308.

(44) Datta, D. B. *A Comprehensive Introduction to Membrane Biochemistry*; Floral Publishing: Madison, WI, 1987.
(45) Connor, J.; Yatvin, M. B.; Huang, L. *Proc. Natl. Acad. Sci. U.S.A.* **1984**, *81*, 1715.
(46) Ellen, H.; Bentz, J.; Szoka, F. C. *Biochemistry* **1985**, *24*, 3099.
(47) Hafez, I. M.; Ansell, S.; Cullis, P. R. *Biophys. J.* **2000**, *79*, 1438.
(48) Tocanne, J.-F.; Teissie, J. *Biochim. Biophys. Acta* **1990**, *1031*, 111.
(49) Tanaka, T. *Phys. Rev. Lett.* **1978**, *40*, 820.
(50) Janas, V. F.; Rodriguez, F.; Cohen, C. *Macromolecules* **1980**, *13*, 977.
(51) Pelton, R. H.; Pelton, H. M.; Morphesis, A.; Rowell, R. L. *Langmuir* **1989**, *5*, 816.
(52) Ricka, J.; Tanaka, T. *Macromolecules* **1984**, *17*, 2916.
(53) McPhee, W.; Tam, K. C.; Pelton, R. *J. Colloid Interface Sci.* **1993**, *156*, 24.
(54) Pelton, R. H.; Chibante, P. *Colloids Surf.* **1986**, *20*, 247.
(55) Zhou, S.; Chu, B. *J. Phys. Chem. B* **1998**, *102*, 1364.
(56) Hirose, Y.; Amiya, T.; Hirokawa, Y.; Tanaka, T. *Macromolecules* **1987**, *20*, 1342.
(57) Ito, S.; Ogawa, K.; Suzuki, H.; Wang, B.; Yoshida, R.; Kokufuta, E. *Langmuir* **1999**, *15*, 4289.
(58) Ogawa, Y.; Ogawa, K.; Wang, B.; Kokufuta, E. *Langmuir* **2001**, *17*, 2670.
(59) Saunders, B. R.; Crowther, H. M.; Vincent, B. *Macromolecules* **1997**, *30*, 482.

MA011644+